nature photonics

ARTICLES

PUBLISHED ONLINE: 23 MARCH 2015 | DOI: 10.1038/NPHOTON.2015.36

High-efficiency light-emitting devices based on quantum dots with tailored nanostructures

Yixing Yang[1†], Ying Zheng[1†], Weiran Cao[2], Alexandre Titov[1], Jake Hyvonen[1], Jesse R. Manders[1], Jiangeng Xue[2]*, Paul H. Holloway[1,2]* and Lei Qian[1]*

We report a full series of blue, green and red quantum-dot-based light-emitting devices (QD-LEDs), all with high external quantum efficiencies over 10%. We show that the fine nanostructure of quantum dots—especially the composition of the graded intermediate shell and the thickness of the outer shell—plays a very important role in determining QD-LED device performance due to its effects on charge injection, transport and recombination. These simple devices have maximum current and external quantum efficiencies of 63 cd A^{-1} and 14.5% for green QD-LEDs, 15 cd A^{-1} and 12.0% for red devices, and 4.4 cd A^{-1} and 10.7% for blue devices, all of which are well maintained over a wide range of luminances from 10^2 to 10^4 cd m^{-2}. All the QD-LEDs are solution-processed for ease of mass production, and have low turn-on voltages and saturated pure colours. The green and red devices exhibit lifetimes of more than 90,000 and 300,000 h, respectively.

Since their inception about three decades ago[1–3], semiconductor quantum dots have been intensively investigated because of their unique optical properties, including size-controlled tunable emission wavelength (known as the 'quantum confinement effect'), narrow emission spectra, high luminescent efficiency and colloidal-based synthesis process[4–7]. All these attractive characteristics make quantum dots excellent candidates for the development of next-generation display technologies. Quantum dot-based light-emitting diodes (QD-LEDs) have been demonstrated recently, and may offer many advantages over conventional LED and organic LED (OLEDs) technologies in terms of colour purity, stability and production cost, while still achieving similar levels of efficiency. To date, however, the electroluminescence efficiencies of QD-LEDs have remained significantly below those of OLEDs, despite steady progress in recent years[8–17]. Recently, an efficient deep-blue QD-LED has been reported that makes use of solution-processed poly(3,4-ethylenedioxythiophene):polystyrene sulphonate (PEDOT:PSS) and poly(*N*-vinyl carbazole) (PVK) as its hole injection and transport layers (HIL and HTL), respectively, and ZnO nanoparticles as its electron transport layer (ETL), and achieves a maximum external quantum efficiency (η_{EQE}) of 7.1% (ref. 15). The same device structure was also used to achieve a green QD-LED with an η_{EQE} of 12.6% (ref. 17). Highly efficient red QD-LEDs with η_{EQE} = 18–20% have been realized using an inverted device structure containing a vacuum-deposited HIL and HTL[16], and also in another arrangement using a thin insulating layer to obtain an enhanced charge balance[18]. These are the first times that the performances of QD-LEDs have been comparable to those of state-of-the-art phosphorescent OLEDs[19–21].

It is noted that although high efficiencies have been achieved with blue (B), green (G) and red (R) QD-LEDs, these single-colour QD-LEDs, developed by different research groups, commonly involve very different quantum dot preparation procedures (for example, one-pot[14,15,17] and two-pot[16] synthesis approaches) and device architectures (conventional[11,13,15,17] versus inverted[14,16], solution-processed[13,15,17] versus vacuum-deposited[14,16], and with various charge transport layers[11,13,14,16,17]). To reduce the manufacturing complexity required to achieve full-colour displays, it is more desirable to use a common device structure to achieve high efficiency for all three colours. Using the same inverted device structure, η_{EQE} values of 1.7%, 5.8% and 7.3% have been achieved with blue, green and red QD-LEDs, respectively, but these are much lower than the highest values ever reported[14]. Another significant hurdle for the mass production of QD-LED displays is device operating lifetime. The reported lifetimes of current QD-LEDs with an initial brightness of 100 cd m^{-2} are on the order of 100–1,000 h (refs 9,11–14), far below the 10,000 h requirement for display applications[7].

Here, we report a full series of blue, green and red QD-LEDs with η_{EQE} > 10%, made using the same solution-processed device structure (only difference being quantum dots emitting at different wavelengths in the emissive layer). By incorporating our high-quality quantum dots with optimized nanostructure, our blue and green QD-LEDs show η_{EQE} values of 10.7% and 14.5%, respectively, corresponding to current efficiencies (η_A) of 4.4 cd A^{-1} and 63 cd A^{-1}, which are the best performances to date. The red QD-LED has good η_{EQE} and η_A values of 12.0% and 15 cd A^{-1}, respectively. More importantly, the device half-lifetimes for the green and red QD-LEDs have been shown to be over 90,000 h and 300,000 h, respectively, for a brightness of 100 cd m^{-2}, although the blue QD-LEDs still has a relatively short lifetime of only 1,000 h. These QD-LEDs also feature a sub-bandgap electroluminescence with extremely low turn-on voltages (1.5–2.6 V), narrow full-width at half-maximum (FWHM of <30 nm) of the electroluminescence peaks and thus highly saturated pure colours, and high brightness, even at low voltages (<6 V). The outstanding performance and low-cost fabrication potential of these full-colour series QD-LEDs are a critical step towards achieving the commercial realization of QD-LED display technology.

To achieve QD-LEDs with such high performance, it is first necessary to prepare high-quality quantum dots by carefully controlling their nanostructure and composition[22–24]. Although colloidal quantum dots (typically CdSe-based) with high quantum yield and monodispersivity have been widely studied and can be readily synthesized[25,26], QD-LED device performance is also substantially affected by the electronic properties of the quantum

[1]NanoPhotonica Inc., Gainesville, Florida 32601, USA. [2]Department of Materials Science and Engineering, University of Florida, Gainesville, Florida 32611, USA. †These authors contributed equally to this work. *e-mail: lei.qian@nanophotonica.com; pholl@mse.ufl.edu; jxue@mse.ufl.edu

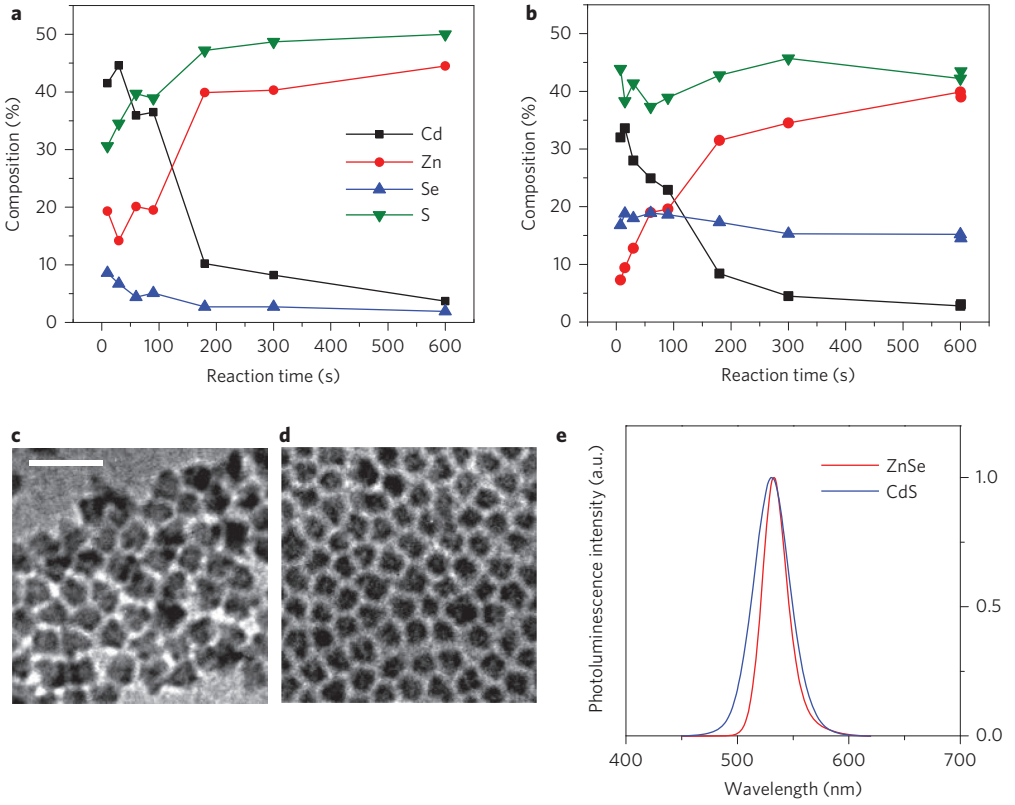

Figure 1 | Surface elemental composition evolution with reaction time by XPS characterization, TEM characterization and photoluminescence spectra of green quantum dots. a, Composition evolution of CdS-rich quantum dots. **b**, Composition evolution of ZnSe-rich quantum dots. **c**, TEM image of CdS-rich quantum dots (scale bar, 25 nm). **d**, TEM image of ZnSe-rich quantum dots (scale bar as in **c**). **e**, Photoluminescence spectra of CdS-rich (blue) and ZnSe-rich (red) quantum dots.

dots[16,27], which in turn are determined by their fine nanostructure. For example, to suppress the nonradiative Auger recombination of charged excitons within a device[16,17,27–29], 'giant' core–shell quantum dots with very thick shells have been developed[27,30] to isolate the surface environment and prevent the accumulation of charge by the quantum dots. However, the efficiency of the QD-LEDs was limited by the moderate quantum yield of these 'giant' quantum dots[24,27]. An alternative approach is to increase the quantum dot layer thickness in contact with the metal-oxide ETL, thereby taking advantage of the ultrafast charge transfer between the quantum dot layer and adjacent ETL to suppress the Auger recombination[16,31,32]. Although these strategies have a variable degree of success in improving the efficiency of QD-LEDs, the thicker quantum dot shell or quantum dot layer is expected to cause an increase in device resistance and therefore require higher driving voltages to obtain the same brightness, thus creating more heat and faster degradation of device performance. So far, none of the QD-LEDs that have high efficiencies have had lifetime test results reported[15–17].

CdS is predominantly used as the outer shell or intermediate layer to form CdSe or CdSe/ZnS multilayer quantum dots[9,11,16,24,27,33]. The Auger recombination process already mentioned mainly originates from the weaker confinement of the electron wavefunction than the corresponding hole in the CdSe/CdS system, leading to a high degree of surface accessibility by photogenerated electrons and leaving the quantum dots in a non-emissive charged state[16,17,27,34,35]. As a result, very thick CdS or ZnS shells are necessary to suppress the Auger recombination process in devices[17,27]. Compared to CdS, ZnSe has a much higher (~0.7 eV) conduction band, although its valence band is only slightly shallower (~0.2 eV; Supplementary Fig. 1)[6,36], providing much better confinement of the electron wavefunction. Hence, thick ZnSe and ZnS shells are not necessarily needed to ensure carrier confinement in the CdSe core. In particular, the thickness of the ZnS outer shell can be reduced significantly to enhance charge injection into QD-LEDs while maintaining high quantum dot quantum yields, thus leading to high efficiency and long lifetime.

Results and discussion

Based on the principles discussed above, we synthesized quantum dots with specially tailored nanostructures using a modified a one-step method[33,37,38]. Our modified method creates quantum dots with a graded, alloyed intermediate shell ($Cd_{1-x}Zn_xSe_{1-y}S_y$) sandwiched between the Cd- and Se-rich core and the Zn- and S-rich outer shell. The gradual change in composition from the core to the outer shell enables effective strain relief caused by lattice mismatch between core and shell, and thus enhances the photoluminescence efficiency of the quantum dots[39]. The composition gradient in the intermediate shell of these quantum dots can be manipulated by varying the relative ratios of Cd and Se precursors. The amounts of Zn and S precursors may also be adjusted to achieve similar photoluminescence emission peak wavelengths and quantum yields for both Cd- and S-rich and Zn- and Se-rich intermediate shell quantum dots (hereafter simply referred to as CdS-rich and ZnSe-rich quantum dots, respectively). The formation of green quantum dots with a CdS-rich and ZnSe-rich intermediate shell can be monitored by X-ray photoelectron spectroscopy (XPS). Figure 1a,b shows the evolution of the surface composition of Cd, Zn, Se and S with growth time for these two types of quantum dot. As shown in Fig. 1a, within a short period, Se is largely consumed for CdSe core nucleation; thereafter, Cd and S components are dominant at the surface, suggesting the formation of a

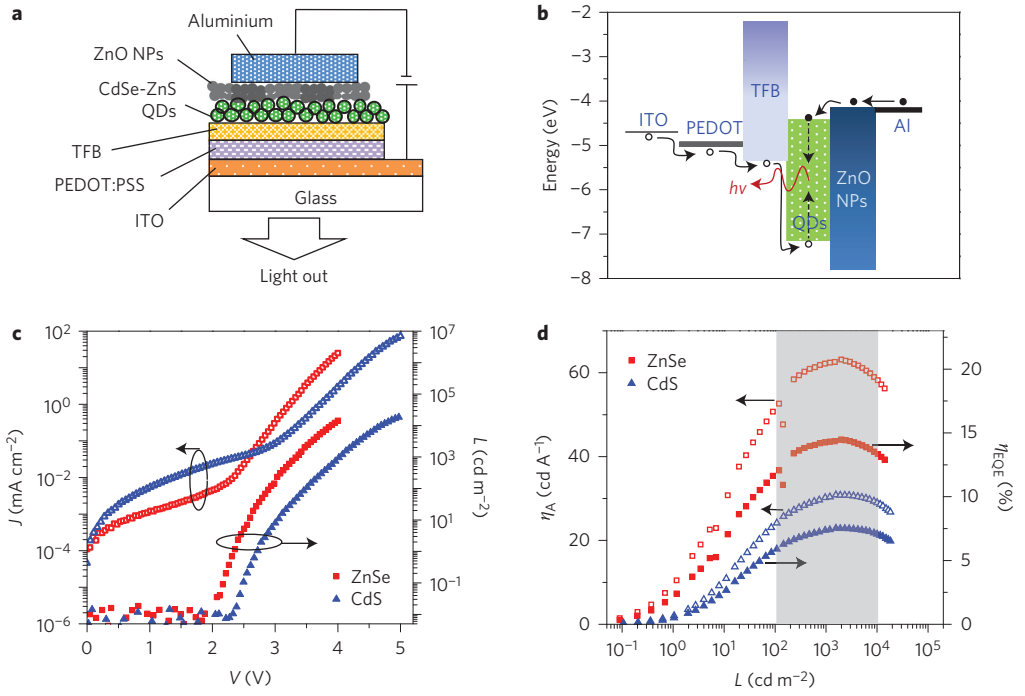

Figure 2 | Schematic of device structure, energy levels and electroluminescence performance of green QD-LEDs. a, Schematic of layers in the device structure. **b**, Energy level diagram for the layers in the device. The migration of holes (open circles) and electrons (filled circles) within the device is shown. **c**, Current density–luminance–voltage (J–L–V) characteristics of the best-performing green QD-LEDs based on CdS-rich (blue triangles) or ZnSe-rich (red squares) intermediate shells. **d**, Current efficiency (η_A) and external quantum efficiency (η_{EQE}) as a function of luminance for the two devices.

CdS-rich intermediate shell. After 2 min reaction, the concentration of Zn quickly rises above that of Cd, signalling the start of the ZnS outer shell growth. As shown in Fig. 1b, for green quantum dots with a ZnSe-rich intermediate shell, the Se composition is much higher and gradually exceeds that of Cd (the concentration of which is reduced by core nucleation), leading to the formation of a ZnSe-rich intermediate shell. In a similar manner, growth of the ZnS outer shell is dominated by reactions at a later time.

Figure 1c,d presents transmission electron microscopy (TEM) images of green quantum dots with CdS-rich and ZnSe-rich intermediate shells, respectively. The average size of CdS-rich green quantum dots was measured to be ~10 nm (with irregular shapes), while the ZnSe-rich quantum dots have a smaller particle size of ~7–8 nm, with high crystallinity (Supplementary Fig. 2) and much better self-assembly characteristics that presumably result from their more regular shapes and better size distribution. The CdS-rich quantum dots have a broader FWHM of photoluminescence emission peak due to their larger particle sizes and wider size distribution, but the two types of green quantum dot have very similar photoluminescence emission peaks at $\lambda = 530$ nm (CdS-rich) and 533 nm (ZnSe-rich), as shown in Fig. 1e. The photoluminescence quantum yields are also very similar, measured to be 70% (CdS-rich) and 75% (ZnSe-rich). It is noted that the core/shell structures for both CdS-rich and ZnSe-rich green quantum dots have been fully optimized for QD-LED efficiency. Hence, the different quantum dot sizes here are consistent with our earlier conclusion that the optimized CdS-rich quantum dots need to have a thicker outer shell to partially suppress Auger recombination. Due to the continuous chemical composition gradient in these one-step synthesized quantum dots, it is difficult to accurately determine the actual thickness of the ZnS outer shell within the quantum dots. However, as the Zn precursor is always in excess, the relative amount of S to Zn precursors (S/Zn%, by molar ratio) can be used to approximate the relative ZnS outer shell thickness. The S/Zn% for optimized CdS-rich and ZnSe-rich green quantum dots are 87% and 50%, respectively, indicating that the ZnS outer shell thickness of ZnSe-rich quantum dots can be estimated to be over 40% thinner than those of CdS-rich quantum dots.

The device structure of a QD-LED is shown schematically in Fig. 2a, and consists of an indium–tin oxide (ITO) transparent anode on a glass substrate, a PEDOT:PSS HIL, a poly(9,9-dioctylfluorene-co-*N*-(4-(3-methylpropyl))diphenylamine) (TFB) HTL, quantum dots as the emissive layer, an ETL of ZnO nanoparticles and an Al cathode. We have already reported this ZnO nanoparticle-based QD-LED device structure, which features all-solution processing with orthogonal solvents (other than the Al cathode) and enhanced charge injection and device stability originating from the ZnO nanoparticles[13]. According to the schematic energy level diagram shown in Fig. 2b, with its electron affinity of ~4.3 eV and ionization potential of ~7.6 eV, the ZnO nanoparticle layer enables efficient electron injection from the Al cathode into the quantum dots, and helps confine holes within the quantum dot layer due to the valence band offset at the quantum dot/ZnO nanoparticle interface, leading to a good charge recombination efficiency. As a stable oxide, ZnO nanoparticles can also provide additional protection to prevent oxygen and water from diffusing into the active layer.

Current density–luminance–voltage (J–L–V) characteristics of QD-LEDs based on the CdS-rich and ZnSe-rich green quantum dots are presented in Fig. 2c. The ZnSe-rich quantum dot-based device exhibits much lower leakage current (at $V < 2$ V) and much higher injection current density at $V > 3$ V than the CdS-rich quantum dot-based device. This can be attributed to the thinner ZnS outer shell of ZnSe-rich quantum dots, which enables better charge injection into the emissive quantum dot layer. The luminance at $V = 4$ V for the ZnSe-rich quantum dot device is $L = 14{,}000$ cd m^{-2}, more than one order of magnitude higher than that of the CdS-rich quantum dot device ($L \approx 800$ cd m^{-2}). The driving voltages required for the ZnSe-rich quantum dot device are only 2.9 to 3.3 V to achieve a luminance of 100 to

Table 1 | Summary of electroluminescence emission peak wavelength λ_{max}, FWHM, turn-on voltage V_T, external quantum efficiency η_{EQE}, power efficiency η_P and current efficiency η_A of optimized blue, green (CdS-rich and ZnSe-rich) and red best-performing QD-LEDs.

Colour of QLEDs	λ_{max} (nm)	FWHM (nm)	V_T (V)	η_{EQE} (%)		η_P (lm W^{-1})		η_A (cd A^{-1})	
				Peak	at 1,000 cd m^{-2}	Peak	at 1,000 cd m^{-2}	Peak	at 1,000 cd m^{-2}
Green (CdS-rich)	534	38	2.2	7.5	7.4	24	23	31	30
Green (ZnSe-rich)	537	29	2.0	14.5	14.3	60	58	63	62
Blue	455	20	2.6	10.7	10.3	2.7	2.7	4.4	4.3
Red	625	25	1.5	12.0	12.0	18	17	15	15

1,000 cd m^{-2}, whereas the turn-on voltage (V_T) is as low as 2.0 eV, suggesting efficient injection of holes and electrons into the quantum dot layer at low driving voltages. For the CdS-rich quantum dot device, V_T is 0.2 eV higher. As shown in Fig. 2b, a considerable hole injection barrier exists at the HTL/quantum dot interface due to the deep-lying valence band of quantum dots, whereas no appreciable electron injection barrier is present at the quantum dot/ETL interface[17]. Therefore, the turn-on voltage is strongly affected by the hole injection barrier. As the valence band of ZnSe is 0.2 eV higher than that of CdS, the hole injection barrier is reduced with a ZnSe-rich intermediate shell, leading to a slightly lower V_T for the ZnSe-rich quantum dot device. It is also noted that the values of V_T for both green QD-LEDs are lower here than the corresponding photon voltage (defined as the photon energy hv divided by the electron charge e, which is 2.3 V for 534 nm or 537 nm emission). This sub-bandgap electroluminescence from QD-LEDs has previously been attributed to an Auger-assisted energy upconversion[40,41].

The current efficiency (η_A) and external quantum efficiency (η_{EQE}) as a function of luminance for both green QD-LEDs are shown in Fig. 2d. A maximum η_A of 31 cd A^{-1} and η_{EQE} of 7.5% are achieved with the CdS-rich quantum dot device at $L \approx 10^3$ cd m^{-2}, and the efficiencies are well maintained within 90% of the maximum values when the luminance is increased to $L \approx 10^4$ cd m^{-2}. Such efficiencies are already among the highest reported for green QD-LEDs. An almost twofold increase in these efficiencies is achieved with the ZnSe-rich quantum dots, with a maximum η_A of 63 cd A^{-1} and η_{EQE} of 14.5%. This is the highest-performance green QD-LED reported to date and is approaching that of state-of-the-art phosphorescent green OLEDs. The reproducibility of this high performance was demonstrated by testing over 70 devices from multiple batches, yielding an average η_A of 59.6 cd A^{-1} (Supplementary Fig. 3). Note that the peak efficiencies of the ZnSe-rich quantum dot device are achieved at $L \approx 10^3$ cd m^{-2}, and high efficiencies ($\eta_A > 50$ cd A^{-1}) are maintained in the range of $L = 10^2$ to 10^4 cd m^{-2}. These characteristics are highly desirable for practical applications such as displays and lighting. Table 1 summarizes the detailed performance parameters for these two types of green QD-LED.

Following the same design principles, we also synthesized red quantum dots with a ZnSe-rich intermediate layer and an ultrathin ZnS outer shell. As above, the relative amounts of S and Zn

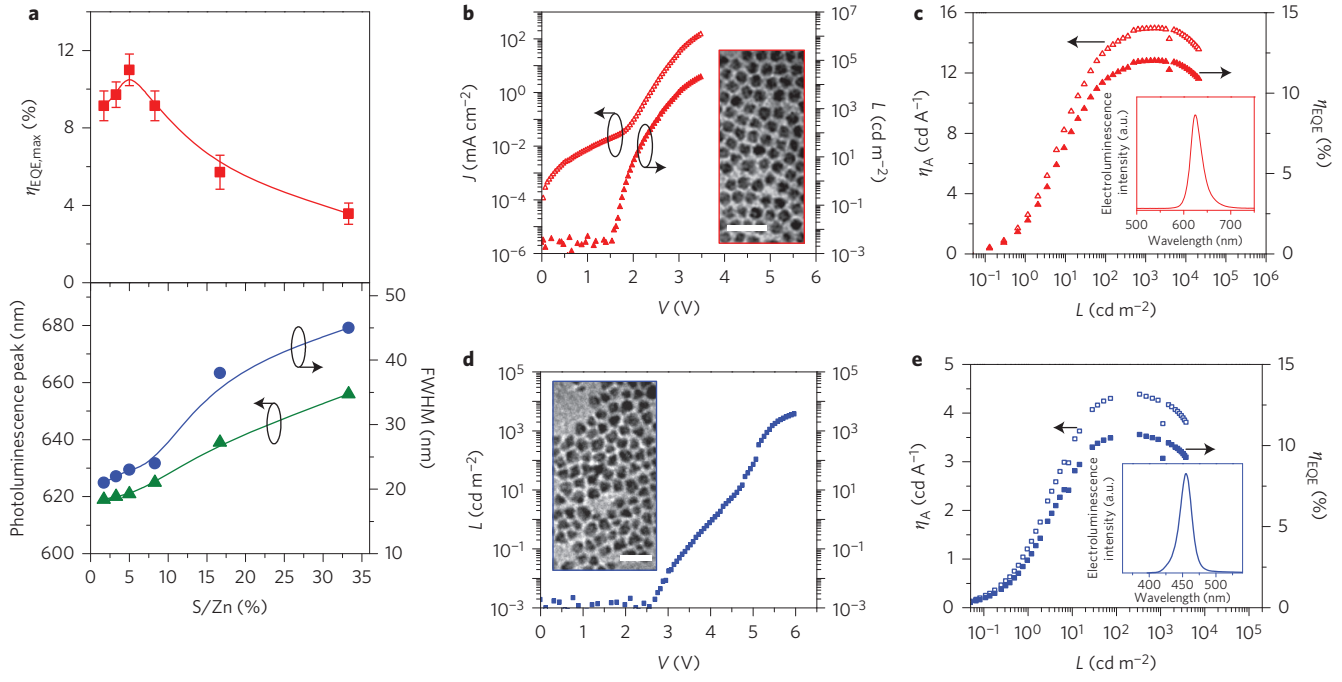

Figure 3 | Electroluminescence performance of red and deep blue QD-LEDs. a, External quantum efficiencies (η_{EQE}) of red QD-LEDs, photoluminescence emission peak wavelengths and FWHM of corresponding red quantum dots with ZnSe-rich intermediate shell versus the relative ratios of S and Zn precursors (S/Zn%). **b**, *J*–*L*–*V* characteristics of the best-performing red QD-LED based on quantum dots with a ZnSe-rich intermediate shell. Inset: TEM image of red quantum dots with a ZnSe-rich intermediate shell (scale bar, 25 nm). **c**, Current efficiency (η_A) and η_{EQE} as a function of luminance of the best-performing red QD-LED based on quantum dots with a ZnSe-rich intermediate shell. Inset: normalized electroluminescence spectrum of the red QD-LED. **d**, *L*–*V* characteristics of the best-performing blue QD-LED. Inset: TEM image of blue quantum dots (scale bar, 25 nm). **e**, η_A and η_{EQE} as a function of luminance of the best-performing blue QD-LED. Inset: normalized electroluminescence spectrum of the blue QD-LED.

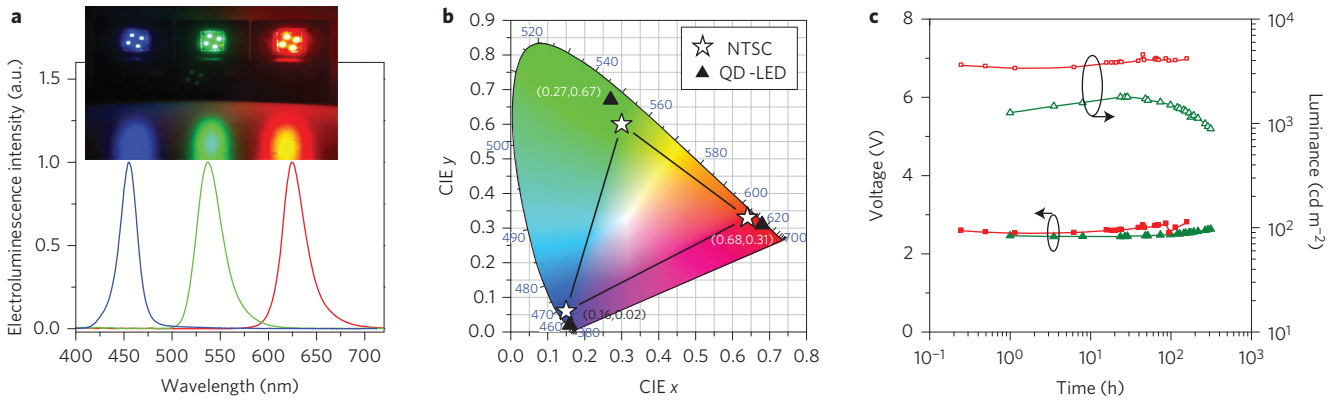

Figure 4 | Electroluminescence spectra, CIE coordinates and operating lifetime of QD-LEDs. a, Normalized electroluminescence spectra and images of blue, green and red QD-LEDs. **b**, CIE coordinates of the three QD-LEDs (triangles) compared to the NTSC colour standards (stars). **c**, Luminance and driving voltage for green (triangles) and red (squares) QD-LEDs versus time of operation under ambient conditions with constant driving currents of 3 and 25 mA cm^{-2}, respectively.

precursors, S/Zn%, can be used to estimate the relative ZnS outer shell thickness. As shown in Fig. 3a, with increasing S/Zn ratio, or ZnS outer shell thickness, the photoluminescence peak of the red quantum dots is gradually redshifted from 619 nm to 656 nm, accompanied by an increase in FWHM from 21 nm to 45 nm. On the other hand, the peak η_{EQE} of the resulting red QD-LEDs exhibit a maximum value with a S/Zn ratio of 5%. This can be explained by the fact that a thinner ZnS outer shell leads to a lower quantum dot photoluminescence quantum yield and deteriorating charge confinement in the quantum dots, whereas a thicker ZnS outer shell leads to decreased charge injection into the quantum dot layer, both of which produce lower efficiencies. The average size of the red quantum dots (corresponding to a 5% S/Zn ratio) was measured to be ~8 nm from the TEM image shown in the inset of Fig. 3b, almost the same as the ZnSe-rich green quantum dots discussed earlier. Considering the larger CdSe core in red quantum dots than in green quantum dots (where the ZnS outer shell is already thin), we can expect the ZnS outer shell of such red quantum dots to be even thinner.

The *J*–*L*–*V* characteristics of QD-LEDs based on red quantum dots with a ZnSe-rich intermediate shell and ultrathin ZnS outer shell are shown in Fig. 3b. Similar to green QD-LEDs, the red device also exhibits sub-bandgap electroluminescence with a very low V_T of only 1.5 V. A maximum luminance of 21,000 cd m^{-2} is achieved with a low driving voltage of $V = 3.5$ V. As shown in Fig. 3c, with the electroluminescence emission wavelength peaked at $\lambda = 625$ nm, the red QD-LEDs have a maximum η_A of 15 cd A^{-1} and η_{EQE} of 12.0% at $L \approx 10^3$ cd m^{-2}, with more than 90% of the maximum efficiency maintained in the range of $L = 10^2$ to 10^4 cd m^{-2}. As a comparison, the red QD-LEDs based on CdS-rich quantum dots have a much lower electroluminescence performance (maximum of $\eta_A = 5.2$ cd A^{-1} and $\eta_{EQE} = 5.4\%$) (Supplementary Fig. 4 and Supplementary Table 1).

To achieve deep blue (peak wavelength of ~450 nm) emission with high photoluminescence efficiency, the CdSe core structure used in green and red quantum dots was modified to $Cd_{1-x}Zn_xS$, which has a larger bandgap than CdSe, with ZnS still used for the outer shell[14,37]. The $Cd_{1-x}Zn_xS$ core has intrinsically better electron wavefunction confinement than the CdSe/CdS system, and will therefore suppress the nonradiative Auger recombination process in a similar way to the CdSe/ZnSe system. The ZnS outer shell of the blue quantum dots was also optimized to be thinner than the thickness previously reported, with an average particle size of ~8 nm, as shown in the inset of Fig. 3d. The luminance–voltage (*L*–*V*) characteristics of QD-LEDs with optimized blue quantum dots with controlled nanostructures are shown in Fig. 3d. Here, PVK was used as the HTL instead of TFB, to obtain enhanced charge balance and efficiency in the blue devices (Supplementary Fig. 6). A comparison of blue QD-LEDs based on PVK and TFB as the HTL is provided in Supplementary Fig. 7 and Supplementary Table 2. Not surprisingly, the blue QD-LED exhibits good electroluminescence performance, with a sub-bandgap turn-on voltage of 2.6 V and a maximum luminance of 4,000 cd m^{-2} at 6 V. The QD-LED emits highly pure deep blue emission with a peak wavelength at $\lambda = 455$ nm and FWHM of only 20 nm, as shown in the inset of Fig. 3e. A maximum η_{EQE} of 10.7% and η_A of 4.4 cd A^{-1} were achieved at $L \approx 10^2$ to 10^3 cd m^{-2} and, again, little efficiency loss (<20%) was observed when the device brightness was extended to $L \approx 10^2$ to 10^4 cd m^{-2}.

Figure 4a shows the normalized electroluminescence spectra of blue, green and red QD-LEDs together with photographs of devices fabricated on 1 inch^2 substrates under operation. With emission wavelength peaks at $\lambda = 455$ nm, 537 nm and 625 nm, the FWHM is less than 30 nm for all colours (Table 1). All devices exhibit very saturated and pure colours, as demonstrated by the Commission Internationale de l'Eclairage (CIE) chromaticity diagram shown in Fig. 4b. The National Television System Committee (NTSC) standard colour triangle is completely covered by the colour gamut of full colour QD-LEDs.

To evaluate the stability of QD-LEDs, the operating lifetimes of the devices were tested under ambient conditions with a typical room temperature of ~23–26 °C and relative humidity of ~30–60%. All devices were encapsulated in commercially available ultraviolet-curing epoxy and cover glass. The luminance and driving voltage versus time for green QD-LEDs under a constant driving current of ~3 mA cm^{-2} are shown in Fig. 4c. Initially, the luminance is $L \approx 1{,}200$ cd m^{-2}, but it increases to $L \approx 1{,}800$ cd m^{-2} within 10 h, probably due to passivation of surface trap states on quantum dots by adsorbed oxygen and water[13,42–44], after which it slowly decreases with operation time, reaching 900 cd m^{-2} after 320 h. Meanwhile, the driving voltages are only slightly increased from 2.4 V to 2.6 V. The half lifetime T_{50} at an initial brightness of 100 cd m^{-2} can then be extrapolated to >90,000 h in accordance with a previously reported method (see Supplementary Section 'Device lifetime test')[45]. The red QD-LEDs were also tested under accelerated conditions and had an even higher initial brightness of ~4,000 cd m^{-2} (Fig. 4c), exhibiting almost no decay in luminance for over 200 h. Instead of gradual device degradation, the red QD-LED was observed to fail suddenly due to delamination of the Al electrode under such stressed test conditions. Even so, the

Figure 5 | Monochrome active matrix QD-LED display prototypes. Electroluminescence images of the 4.3-inch red and green active matrix QD-LED display prototypes with a resolution of 480 × 800 using an LTPS TFT backplane.

extrapolated lifetime of red QD-LEDs under 100 cd m^{-2} is still more than 300,000 h. The excellent operating lifetimes of green and red QD-LEDs well exceed the 10,000 h requirement of display applications[7], which can be mainly attributed to the extremely low driving voltages induced by the efficient and balanced charge injection/transport and charge recombination within the devices, as well as the effective protection provided by the stable ZnO ETL. However, the blue QD-LEDs still have a much lower lifetime of only 1,000 h, probably due to the higher injection energy barriers for both electrons and holes, which lead to higher driving voltages and potential nonradiative recombination at the interfaces. Nevertheless, our blue devices are still the most efficient and stable blue QD-LEDs reported to date.

As a preliminary demonstration towards the practical application of QD-LEDs in full-colour displays, monochrome active matrix (AM) QD-LED display prototypes were fabricated using the spin-coating process. Figure 5 presents images of 4.3-inch (diagonal) red and green AM QD-LED display prototypes with a resolution of 480 × 800 on low-temperature poly-silicon (LTPS) thin-film transistor (TFT) backplanes. Advanced printing technologies, such as micro-contact printing[12,46] and ink-jet printing[47], are probably needed to create pixelated full-colour QD-LED displays with sufficient image quality and a reliable production process.

Conclusion

In summary, we have demonstrated high performance in both device efficiency and lifetime for red, green and blue QD-LEDs. The detailed nanostructure of the quantum dots, including the composition of the intermediate shell and the thickness of the outer shell, is found to be of great importance to achieving such high-performance QD-LEDs. The high-quality quantum dots prepared here not only exhibit high photoluminescence efficiencies and narrow emission peaks, but have tailored nanostructures to maximize the efficiencies of charge injection/transport and radiative charge recombination. The similar device architecture used for all three (red, blue, green) high-performance QD-LEDs is anticipated to greatly reduce the fabrication complexity of full-colour QD-LED displays, and the demonstration of mobile-device-sized monochrome AM QD-LED prototypes is further evidence for the practical applicability of the QD-LEDs. We believe that the work presented in this Article is an important step towards the realization of full-colour QD-LEDs displays.

Methods

Materials synthesis. The blue, green and red quantum dots used here were prepared according to methods reported previously in the literature, with appropriate modifications[33,37]. Specific details of the methods used in this work are provided in the Supplementary Information.

ZnO nanoparticles were synthesized using a solution-precipitation process as reported in the literature[13]. For a typical synthesis, a solution of zinc acetate in dimethyl sulphoxide (DMSO, 0.5 M) and 30 ml of a solution of tetramethylammonium hydroxide (TMAH) in ethanol (0.55 M) were mixed and stirred for 1 h in ambient air, then washed and dispersed in ethanol for device fabrication.

Device fabrication. QD-LEDs were fabricated by spin coating on glass substrates that were commercially pre-coated with an indium–tin oxide anode (sheet resistance ~20 Ω $\square^{-1}$). The substrates were cleaned consecutively in ultrasonic baths of deionized water, acetone and 2-propanol for 15 min each, and were then exposed to

an ultraviolet ozone ambient for 15 min. The substrates were spin coated with PEDOT:PSS (AI 4083) and baked at 150 °C for 15 min in air. The coated substrates were then transferred into a N_2-filled glove box for spin coating of layers of TFB or PVK, quantum dots and ZnO nanoparticles. TFB was purchased from American Dye Source and PVK from Sigma Aldrich, and both were used as supplied. The TFB or PVK layers were spin coated at 4,000 r.p.m. for 30 s using an 8 mg ml^{-1} solution in chlorobenzene, followed by baking at 150 °C for 30 min. Quantum dots and ZnO nanoparticle layers were then spin coated and baked at 70 °C for 30 min. The optimized quantum dot layer thicknesses were ~20 nm for green (18 mg ml^{-1} quantum dot solution, 2,000 r.p.m. spin speed), ~16 nm for red (15 mg ml^{-1}, 2,500 r.p.m.) and ~20 nm for blue (18 mg ml^{-1}, 2,000 r.p.m.), as determined from an efficiency comparison of devices with various quantum dot layer thicknesses. The thickness of the ZnO nanoparticle layer was optimized by varying both the concentration of the ZnO nanoparticle solution and the spin speed of the spin coating process. In accordance with the microcavity effect, the optimized ZnO layer thickness is different for specific colour-emitting QD-LEDs and is proportional to the emitting wavelength of a device. The short-wavelength-emitting blue QD-LEDs therefore have the thinnest optimized ZnO layer thickness of ~30 nm (30 mg ml^{-1} ZnO solution, 4,000 r.p.m. spin speed), while those for the longer-wavelength-emitting green and red QD-LEDs are ~40 nm (50 mg ml^{-1}, 2,000 r.p.m.) and ~65 nm (60 mg ml^{-1}, 1,500 r.p.m.), respectively. Similar to optimization of the quantum dot layer thickness, the optimized ZnO layer thickness for each device was determined by an efficiency comparison of devices with various ZnO layer thicknesses. Finally, the multilayer samples were loaded into a high-vacuum chamber (base pressure of ~1×10^{-7} torr) for deposition of an Al cathode (100 nm), patterned by an *in situ* shadow mask to form an active device area of 4 mm^2. All devices were encapsulated in commercially available ultraviolet-curing epoxy and cover glass to protect the devices from oxygen and water.

Characterization and instrumentation. Photoluminescence spectra were obtained in CH_2Cl_2 solutions with a JASCO FP750 spectrometer by excitation at the absorption maxima. The size of the as-synthesized quantum dots was characterized using a JEM-2010F transmission electron microscope (TEM) with 200 keV electron beam energy. Samples for TEM were prepared on a 230-mesh copper grid coated with an ultra-thin carbon supporting film (Beijing Zhongjingkeyi Technology). XPS data were collected with a PHI 5000 VersaProbe X-ray photoelectron spectrometer using monochromatic X-rays from an Al anode. High-resolution data were collected from the region around Cd 3*d*, S 2*p*, Se 3*d* and Zn 2*p*. The *J*–*L*–*V* characteristics of the QD-LEDs were measured under ambient conditions using an Agilent 4155C semiconductor parameter analyser and a calibrated silicon detector (Newport 818 UV). Luminance was calibrated using a Minolta luminance meter (LS-100) according to the suggested method[48]. Electroluminescence spectra were taken using an OcenaOptics HR4000 spectrometer with the devices driven at a constant current using a Keithley 2400 source meter.

Received 1 October 2014; accepted 10 February 2015; published online 23 March 2015

References

1. Ekimov, A. I. & Onushchenko, A. A. Quantum size effect in 3-dimensional microscopic semiconductor crystals. *J. Exp. Theor. Phys. Lett.* **34,** 345–349 (1981).
2. Efros, A. L. Interband absorption of light in a semiconductor sphere. *Sov. Phys. Semicond.* **16,** 772–775 (1982).
3. Brus, L. E. A simple model for the ionization potential, electron affinity, and aqueous redox potentials of small semiconductor crystallites. *J. Chem. Phys.* **79,** 5566–5571 (1983).
4. Brus, L. Electronic wave-functions in semiconductor clusters—experiment and theory. *J. Phys. Chem.* **90,** 2555–2560 (1986).
5. Alivisatos, A. P. Semiconductor clusters, nanocrystals, and quantum dots. *Science* **271,** 933–937 (1996).
6. Lim, J. *et al.* Perspective on synthesis, device structures, and printing processes for quantum dot displays. *Opt. Mater. Express* **2,** 594–628 (2012).
7. Shirasaki, Y., Supran, G. J., Bawendi, M. G. & Bulovic, V. Emergence of colloidal quantum-dot light-emitting technologies. *Nature Photon.* **7,** 13–23 (2012).
8. Coe, S., Woo, W. K., Bawendi, M. & Bulovic, V. Electroluminescence from single monolayers of nanocrystals in molecular organic devices. *Nature* **420,** 800–803 (2002).
9. Sun, Q. *et al.* Bright, multicoloured light-emitting diodes based on quantum dots. *Nature Photon.* **1,** 717–722 (2007).
10. Caruge, J. M., Halpert, J. E., Wood, V., Bulovic, V. & Bawendi, M. G. Colloidal quantum-dot light-emitting diodes with metal-oxide charge transport layers. *Nature Photon.* **2,** 247–250 (2008).
11. Cho, K. S. *et al.* High-performance crosslinked colloidal quantum-dot light-emitting diodes. *Nature Photon.* **3,** 341–345 (2009).
12. Kim, T. H. *et al.* Full-colour quantum dot displays fabricated by transfer printing. *Nature Photon.* **5,** 176–182 (2011).
13. Qian, L., Zheng, Y., Xue, J. & Holloway, P. H. Stable and efficient quantum-dot light-emitting diodes based on solution-processed multilayer structures. *Nature Photon.* **5,** 543–548 (2011).
14. Kwak, J. *et al.* Bright and efficient full-color colloidal quantum dot light-emitting diodes using an inverted device structure. *Nano Lett.* **12,** 2362–2366 (2012).
15. Lee, K. H. *et al.* Highly efficient, color-pure, color-stable blue quantum dot light-emitting devices. *ACS Nano* **7,** 7295–7302 (2013).
16. Mashford, B. S. *et al.* High-efficiency quantum-dot light-emitting devices with enhanced charge injection. *Nature Photon.* **7,** 407–412 (2013).
17. Lee, K. H. *et al.* Over 40 cd/A efficient green quantum dot electroluminescent device comprising uniquely large-sized quantum dots. *ACS Nano* **8,** 4893–4901 (2014).
18. Dai, X. *et al.* Solution-processed, high-performance light-emitting diodes based on quantum dots. *Nature* **515,** 86–89 (2014).
19. Adachi, C., Baldo, M. A., Thompson, M. E. & Forrest, S. R. Nearly 100% internal phosphorescence efficiency in an organic light-emitting device. *J. Appl. Phys.* **90,** 5048–5051 (2001).
20. Baldo, M. A., Lamansky, S., Burrows, P. E., Thompson, M. E. & Forrest, S. R. Very high-efficiency green organic light-emitting devices based on electrophosphorescence. *Appl. Phys. Lett.* **75,** 4–6 (1999).
21. Baldo, M. A. *et al.* Highly efficient phosphorescent emission from organic electroluminescent devices. *Nature* **395,** 151–154 (1998).
22. Wang, X. *et al.* Non-blinking semiconductor nanocrystals. *Nature* **459,** 686–689 (2009).
23. Mahler, B. *et al.* Towards non-blinking colloidal quantum dots. *Nature Mater.* **7,** 659–664 (2008).
24. Chen, O. *et al.* Compact high-quality CdSe–CdS core–shell nanocrystals with narrow emission linewidths and suppressed blinking. *Nature Mater.* **12,** 445–451 (2013).
25. Li, J. *et al.* Large-scale synthesis of nearly monodisperse CdSe/CdS core/shell nanocrystals using air-stable reagents via successive ion layer adsorption and reaction. *J. Am. Chem. Soc.* **125,** 12567–12575 (2003).
26. Shen, H. *et al.* High quality synthesis of monodisperse zinc-blende CdSe and CdSe/ZnS nanocrystals with a phosphine-free method. *CrystEngComm* **11,** 1733–1738 (2009).
27. Pal, B. N. *et al.* 'Giant' CdSe/CdS core/chell nanocrystal quantum dots as efficient electroluminescent materials: strong influence of shell thickness on light-emitting diode performance. *Nano Lett.* **12,** 331–336 (2011).
28. Jha, P. P. & Guyot-Sionnest, P. Photoluminescence switching of charged quantum dot films. *J. Phys. Chem. C* **111,** 15440–15445 (2007).
29. Woo, W. K. *et al.* Reversible charging of CdSe nanocrystals in a simple solid-state device. *Adv. Mater.* **14,** 1068–1071 (2002).
30. Htoon, H. *et al.* Highly emissive multiexcitons in steady-state photoluminescence of individual 'giant' CdSe/CdS core/shell nanocrystals. *Nano Lett.* **10,** 2401–2407 (2010).
31. Jin, S., Song, N. & Lian, T. Suppressed blinking dynamics of single QDs on ITO. *ACS Nano* **4,** 1545–1552 (2010).
32. Wu, X. & Yeow, E. K. L. Charge-transfer processes in single CdSe/ZnS quantum dots with p-type NiO nanoparticles. *Chem. Commun.* **46,** 4390–4392 (2010).
33. Bae, W. K., Char, K., Hur, H. & Lee, S. Single-step synthesis of quantum dots with chemical composition gradients. *Chem. Mater.* **20,** 531–539 (2008).
34. Li, S., Steigerwald, M. L. & Brus, L. E. Surface states in the photoionization of high-quality CdSe core/shell nanocrystals. *ACS Nano* **3,** 1267–1273 (2009).
35. Cherniavskaya, O., Chen, L. W., Islam, M. A. & Brus, L. Photoionization of individual CdSe/CdS core/shell nanocrystals on silicon with 2-nm oxide depends on surface band bending. *Nano Lett.* **3,** 497–501 (2003).
36. Wei, S. & Zunger, A. Calculated natural band offsets of all II–VI and III–V semiconductors: chemical trends and the role of cation *d* orbitals. *Appl. Phys. Lett.* **72,** 2011–2013 (1998).
37. Bae, W. K., Nam, M. K., Char, K. & Lee, S. Gram-scale one-pot synthesis of highly luminescent blue emitting $Cd_{1-x}Zn_xS$/ZnS nanocrystals. *Chem. Mater.* **20,** 5307–5313 (2008).
38. Bae, W. K. *et al.* Highly efficient green-light-emitting diodes based on CdSe@ZnS quantum dots with a chemical-composition gradient. *Adv. Mater.* **21,** 1690–1694 (2009).
39. Dabbousi, B. O. *et al.* (CdSe)ZnS core–shell quantum dots: synthesis and characterization of a size series of highly luminescent nanocrystallites. *J. Phys. Chem. B* **101,** 9463–9475 (1997).
40. Qian, L. *et al.* Electroluminescence from light-emitting polymer/ZnO nanoparticle heterojunctions at sub-bandgap voltages. *Nano Today* **5,** 384–389 (2010).
41. Pandey, A. K. & Nunzi, J. M. Rubrene/fullerene heterostructures with a half-gap electroluminescence threshold and large photovoltage. *Adv. Mater.* **19,** 3613–3617 (2007).
42. Pechstedt, K., Whittle, T., Baumberg, J. & Melvin, T. Photoluminescence of colloidal CdSe/ZnS quantum dots: the critical effect of water molecules. *J. Phys. Chem. C* **114,** 12069–12077 (2010).
43. Cordero, S. R., Carson, P. J., Estabrook, R. A., Strouse, G. F. & Buratto, S. K. Photo-activated luminescence of CdSe quantum dot monolayers. *J. Phys. Chem. B* **104,** 12137–12142 (2000).
44. Dembski, S. *et al.* Photoactivation of CdSe/ZnS quantum dots embedded in silica colloids. *Small* **4,** 1516–1526 (2008).

45. Zhang, J., Li, D., Wu, W., Wu, H. & Zhu, W. Lifetime prediction of white OLED based on MLE under lognormal distribution. *J. Test. Eval.* **41,** 398–402 (2013).
46. Kim, L. *et al.* Contact printing of quantum dot light-emitting devices. *Nano Lett.* **8,** 4513–4517 (2008).
47. Haverinen, H. M., Myllyla, R. A. & Jabbour, G. E. Inkjet printed RGB quantum dot-hybrid LED. *J. Disp. Technol.* **6,** 87–89 (2010).
48. Forrest, S. R., Bradley, D. D. C. & Thompson, M. E. Measuring the efficiency of organic light-emitting devices. *Adv. Mater.* **15,** 1043–1048 (2003).

Acknowledgements

This work was supported financially by the US National Science Foundation (NSF; SBIR Phase I award no. 1248863 and Phase II award no. 1353411) and the Florida High-Tech Corridor Council (FHTCC). Assistance with data collection and reduction by R. Zhou and J. Mudrick (Materials Science and Engineering, University of Florida) is acknowledged. The authors also acknowledge Shanghai Tianma Micro-Electronics Group for assistance with AM QD-LED fabrication. J.X. acknowledges financial support from the NSF Major Research Instrumentation Program for the acquisition of the PHI XPS instrument.

Author contributions

Y.Y. and Y.Z. synthesized material, fabricated devices, collected performance data and postulated mechanisms to explain the performance of the QD-LEDs. W.C. carried out the TEM and XPS measurements. A.T. and J.H. carried out the lifetime test and fabrication of the 4.3-inch AM QD-LED prototypes. J.R.M. carried out the XRD measurement and device efficiency distribution statistics. J.X., P.H.H. and L.Q. supervised the synthesis of materials and devices, directed the collection of performance data, designed tests for the postulated mechanism, and finalized the manuscript.

Additional information

Supplementary information is available in the online version of the paper. Reprints and permissions information is available online at www.nature.com/reprints. Correspondence and requests for materials should be addressed to J.X., P.H.H. and L.Q.

Competing financial interests

The authors declare competing financial interests. Y.Y., A.T., J.H. and J.R.M. are employees of NanoPhotonica Inc., and Y.Z. and L.Q. are Founders of NanoPhotonica Inc., which is the provider of the QD-LEDs display technique and related materials.